Optimal Design of a Surface Mounted Permanent-Magnet BLDC Motor for Spacecraft Applications

R.P. Praveen[1], M.H. Ravichandran[2], V.T. Sadasivan Achari[3], Dr. V.P. Jagathy Raj[4], Dr. G. Madhu[5], Dr. G.R. Bindu[6], and Dr. F. Dubas[7]

***Abstract*— This paper presents the optimal design of a surface mounted permanent-magnet (PM) Brushless direct-current (BLDC) motor meant for spacecraft applications. The spacecraft applications requires the choice of a motor with high torque density, minimum cogging torque, better positional stability and high torque to inertia ratio. Performance of two types of machine configurations viz Slotted PMBLDC and Slotless PMBLDC with Halbach array are compared with the help of analytical and finite element (FE) methods. It is found that unlike a Slotted PMBLDC motor, the Slotless type with Halbach array develops zero cogging torque without reduction in the developed torque. Moreover, the machine being coreless provides high torque to inertia ratio and zero magnetic stiction.**

***Index Terms*—Brushless DC motor, slotted, slotless, Halbach , torque, cogging, space application**

I. INTRODUCTION

The BLDC motors have been proven to be the best all-around type of motors for aerospace applications because of their long life, high torque, high efficiency, and low heat dissipation [1]. The torque produced in a Slotted PMBLDC motor can be classified as alignment torque (i.e., useful torque) and cogging torque. The alignment torque is produced due to the interaction of the PM with the stator conductors and the cogging Torque is caused by the variation of the magnetic energy stored in the air gap, due to the PM flux with the angular position of the rotor. Simply it is due to the interaction between the rotor magnetic flux and the variation of stator [2]. For high performance applications, torque smoothness is essential. Hence, it is very important to consider torque ripple minimization and its related harmonics without affecting the developed torque of the machine. The cogging torque is one of the disadvantages faced in the slotted motor design, as it causes high ripple in the torque generated by the motor.

The Attitude Control Systems (ACS) for future spacecraft applications requires an ideal choice of motor that has high torque density, zero cogging torque, high positional stability, high torque to inertia ratio and zero magnetic stiction. Stepper motors, a special case of BLDC motors cannot be used for critical ACS applications because of its high ripple torque. Moreover the research work carried out by the authors [3] clearly reveals the magnitude of the detent torque present in the stepper motor which is almost 13 % of the developed torque. A slotless BLDC motor design however eliminates the tooth ripple component of cogging as well as has little slot harmonic effects thereby facilitating the need of smooth torque output required for the application. A slotless machine, however suffers from a generally lower magnetic flux crossing the motor air gap which results in a lower power output in the slotless design compared to an equivalent slotted design [4-5]. This reduction in the magnetic flux crossing the air-gap is compensated by the use of Halbach magnetized array having strong and uniform magnetic field. As per the requirements of the spacecraft application the outer diameter and axial length of the machine is selected as 104 mm and 40 mm respectively. Hence a design is to be developed in accordance with the specifications for spacecraft applications.

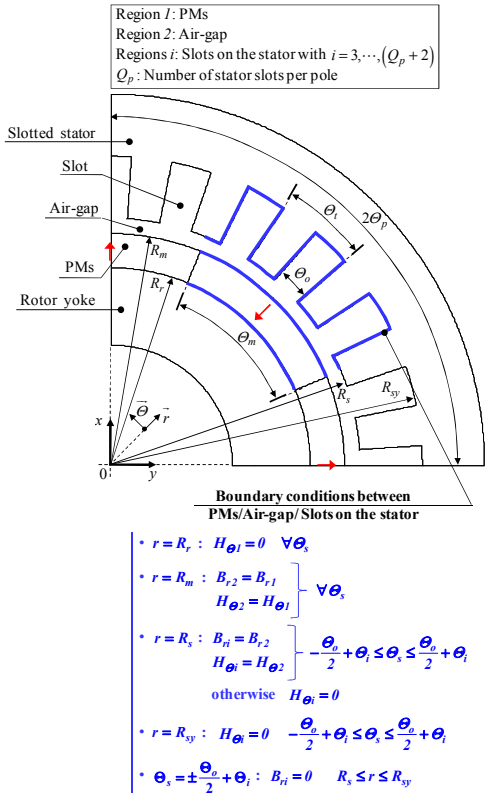

Fig. 1. Cross section of a slotted PMBLDC Motor [6].

II. ANALYSIS OF A SLOTTED PMBLDC MOTOR

A. Analytical Modeling

Fig. 1. shows the cross section of a slotted PMBLDC motor under one pole pitch and is used for the exact analytical solution (i.e., the Maxwell's equation applied in sub-domain)

R.P. Praveen[1] is a Ph.D Research Scholar with Cochin University of Science and Technology, Kerala, India.

M.H. Ravichandran[2] and V.T. Sadasivan Achari[3] are with ISRO Inertial Systems Unit, Trivandrum, Kerala, India.

Dr. V.P. Jagathy Raj[4] and Dr. G. Madhu[5] are with Cochin University of Science and Technology, Kerala, India.

Dr. G.R. Bindu[6] is a Selection Grade Lecturer in the Electrical Department of College of Engineering, University of Kerala, India.

Dr. F. Dubas[7] is with University of Franche-Comte (UFC), FEMTO-ST Institute, ENISYS Department, Belfort, France.

978-1-4244-7926-9/11/$26.00 ©2011 IEEE

of the no load magnetic flux density with the effect of slotting considered.

The main parameters of this geometry are: the radius of the stator yoke surface, R_{sy}, the radius of the stator surface, R_s, the radius of the PMs surface, R_m, the radius of the rotor yoke surface, R_r, the mechanical angle of PMs, Θ_m, the mechanical angle of a stator slot-opening, Θ_o, the mechanical angle of a stator tooth-pitch, Θ_t, and the mechanical angle of a pole-pitch, Θ_p.

The authors make the following assumptions which are usual in many models of the literature. The usual assumptions of all models in the literature are [6]: i) end-effects are neglected; ii) the stator and rotor back-iron is infinitely permeable (i.e., the magnetic saturation is neglected); iii) the electrical conductivity of the PMs is assumed to be null to calculate the no-load magnetic vector potential (i.e., non-resolution of Diffusion's equations); iv) the PMs are assumed to be nonoriented, isotropic, and having a linear demagnetization characteristic (rare earth magnets); v) the stator slot faces are radial as shown in Fig. 1.

The exact analytical model is based on 2-D analysis in polar coordinates. It involves the solution of *Laplace's equations* in the air-gap (i.e., concentric region: Region *2*) and in the slots on the stator (i.e., non-concentric regions: Regions *i*) and the solution of *Poisson's equations* in the PMs (i.e., concentric region: Region *1*) [see Fig. 1] with constant magnetic permeabilities:

$$\Delta A_{z1} = -\frac{\mu_0}{r}\cdot\left(M_\Theta - \frac{\partial M_r}{\partial \Theta_s}\right) \text{ in Region } 1, \tag{1a}$$

$$\Delta A_{z2} = 0 \text{ in Region } 2, \tag{1b}$$

$$\Delta A_{zi} = 0 \text{ in Regions } i \text{ (for } I = 0 \text{ A)}, \tag{1c}$$

where $A_{z1} \sim A_{zi}$ are the no-load magnetic vector potential in different regions, μ_0 is the vacuum permeability, M_r and M_Θ are respectively the radial and tangential components of the magnetization $\overrightarrow{M}$, r and Θ_s are respectively the radial position and the mechanical angular position of the stator (the position $\Theta_s = 0$ is the center of a slot).

By combining (1) with the boundary conditions at the interface between the various regions [see Fig. 1] and by using the method of separating variables, the no-load magnetic vector potential solutions with the slotting effect can be determined in Fourier's series. In [6], the no-load magnetic flux density, in each region, has been compared to the FEA calculations and the agreement was very good considering both amplitude and waveform. The magnetic vector potential as well as the radial and tangential components for the magnetic flux density at no-load are expressed in the PMs (i.e., Region *1*) by

$$A_{z1} = B_{rm}\cdot R_m \cdot f_{z1}\left(r,\Theta_s\right) \ \forall np, \tag{2a}$$

$$B_{r1} = B_{rm}\cdot f_{r1}\left(r,\Theta_s\right) \ \forall np, \tag{2b}$$

$$B_{\Theta 1} = B_{rm}\cdot f_{\Theta 1}\left(r,\Theta_s\right) \ \forall np, \tag{2c}$$

in the air-gap (i.e., in Region *2*) by

$$A_{z2} = B_{rm}\cdot R_m \cdot f_{z2}\left(r,\Theta_s\right) \ \forall np, \tag{3a}$$

$$B_{r2} = B_{rm}\cdot f_{r2}\left(r,\Theta_s\right) \ \forall np, \tag{3b}$$

$$B_{\Theta 2} = B_{rm}\cdot f_{\Theta 2}\left(r,\Theta_s\right) \ \forall np, \tag{3c}$$

in the slots on the stator (i.e., Regions *i*) by

$$A_{zi} = B_{rm}\cdot R_s \cdot f_{zi}\left(r,\Theta_s\right) \ \forall v, \tag{4a}$$

$$B_{ri} = B_{rm}\cdot f_{ri}\left(r,\Theta_s\right) \ \forall v, \tag{4b}$$

$$B_{\Theta i} = B_{rm}\cdot f_{\Theta i}\left(r,\Theta_s\right) \ \forall v, \tag{4c}$$

where B_{rm} is the remanent flux density of PMs; p is the number of pole pairs; n and v are respectively the spatial and the slotting harmonic orders; $f_{z1} \sim f_{\Theta i}$ are the dimensionless functions in Fourier's series which depend respectively on the integration constants E_{1n} & G_{1n} in Region *1*, $E_{2n} \sim H_{2n}$ in Region *2*, and F_{iv} in Regions *i*. These dimensionless functions are completely detailed in [6].

The coefficients E_{1n}, G_{1n}, $E_{2n} \sim H_{2n}$ and F_{iv} are determined by numerically solving the linear equations (i.e., the Cramer's system) for each Θ_{rs} (with Θ_{rs} the mechanical angular position between the rotor and the stator):

$$[IC] = [Q]^{-1}\cdot[K], \tag{5a}$$

$$[IC] = \begin{bmatrix} E_{1n} \\ E_{2n} \\ F_{2n} \\ G_{1n} \\ G_{2n} \\ H_{2n} \\ F_{3v} \\ F_{4v} \\ \vdots \\ F_{(Q_p+2)v} \end{bmatrix} \text{ and } [K] = \begin{bmatrix} K_{1n} \\ K_{3n} \\ 0 \\ K_{2n} \\ K_{4n} \\ 0 \\ 0 \\ 0 \\ \vdots \\ 0 \end{bmatrix}, \tag{5b}$$

$$[Q] = \begin{bmatrix} Q_A & 0 & Q_B \\ 0 & Q_A & Q_C \\ Q_D & Q_E & Q_F \end{bmatrix}, \tag{5c}$$

where

$$Q_A = \begin{bmatrix} Q_{1nn} & Q_{0nn} & Q_{0nn} \\ Q_{2nn} & -Q_{0nn} & Q_{0nn} \\ 0 & Q_{3nn} & Q_{4nn} \end{bmatrix}, \tag{6a}$$

$$Q_B = \begin{bmatrix} 0 & 0 & \cdots & 0 \\ 0 & 0 & \cdots & 0 \\ Q_{5nv3} & Q_{5nv4} & \cdots & Q_{5nv(Q_p+2)} \end{bmatrix}, \tag{6b}$$

$$Q_C = \begin{bmatrix} 0 & 0 & \cdots & 0 \\ 0 & 0 & \cdots & 0 \\ Q_{6nv3} & Q_{6nv4} & \cdots & Q_{6nv(Q_p+2)} \end{bmatrix}, \quad (6c)$$

$$Q_D = \begin{bmatrix} 0 & Q_{7vn3} & Q_{8vn3} \\ 0 & Q_{7vn4} & Q_{8vn4} \\ \vdots & \vdots & \vdots \\ 0 & Q_{7vn(Q_p+2)} & Q_{8vn(Q_p+2)} \end{bmatrix}, \quad (6d)$$

$$Q_E = \begin{bmatrix} 0 & Q_{9vn3} & Q_{10vn3} \\ 0 & Q_{9vn4} & Q_{10vn4} \\ \vdots & \vdots & \vdots \\ 0 & Q_{9vn(Q_p+2)} & Q_{10vn(Q_p+2)} \end{bmatrix}, \quad (6e)$$

$$Q_F = \begin{bmatrix} Q_{11vv3} & 0 & \cdots & 0 \\ 0 & Q_{11vv4} & \cdots & 0 \\ \vdots & \vdots & \ddots & \vdots \\ 0 & 0 & \cdots & Q_{11vv(Q_p+2)} \end{bmatrix}, \quad (6f)$$

with Nn and Nv are the number terms in the Fourier's series for the computation of no-load local quantities, the unit matrix Q_{0nn} has $Nn \times Nn$ coefficients, the diagonal matrices $Q_{1nn} \sim Q_{4nn}$ have $Nn \times Nn$ coefficients, the matrices $Q_{5nvi} \sim Q_{6nvi}$ and $Q_{7vni} \sim Q_{10vni}$ have $Nn \times Nv$ and $Nv \times Nn$ coefficients respectively, the diagonal matrix Q_{11vvi} has $Nv \times Nv$ coefficients, and the matrices $K_{1n} \sim K_{4n}$ have $Nn \times 1$ coefficients which depend on Θ_{rs}. The corresponding elements in the matrices are derived in line with the work of one of the authors [6].

One can note that (5) for each Θ_{rs} consists of $6 \cdot Nn + Q_p \cdot Nv$ equations and unknowns. This 2-D exact analytical model a code was developed in MATHCAD for analyzing the no load magnetic flux density of a slotted PMBLDC motor in all regions.

B. Analytical Results

The closed form solution derived in the previous section is used for designing an experimental radial magnetized Slotted PMBLDC Motor within the dimensional requirements of (104x40) mm for spacecraft applications. The Table 1 shows the design details of the experimental slotted PMBLDC motor with radial magnetized PMs.

Fig.2. shows the radial component for the no load magnetic flux density of the experimental radial magnetized slotted PMBLDC motor under one pole pitch from the 2-D exact analytical model. The experimental slotted motor has 36 slot and teeth combination and the number of stator slots per pole is 3. From Fig.2, it is clear that significant amount of harmonics is present in the magnetic flux density waveform due to the effect of slotting. The basic design parameters obtained from the analytical model is used to model the machine in FE and optimization has to be carried out in FE in order to reduce the cogging component of torque to suit space applications.

TABLE I
DESIGN DETAILS OF THE EXPERIMENTAL SLOTTED PMBLDC MOTOR

Parameter	**Value**
Dimension	Φ(104x 40) mm
Supply voltage	28 V
No. of phases (m)	3
No. of poles ($2p$)	12
No. of slots (Q_s)	36
Resistance/Phase	3.37 Ω
Air-gap thickness	0.5mm
Permanent magnet	Sm_2CO_{17}
Magnet thickness	4 mm
Axial length of PMs	30 mm
Radius of the stator yoke surface (R_{sy})	50.5 mm
Radius of the stator surface (R_s)	44.5 mm
Radius of the PM's surface (R_m)	44 mm
Radius of the rotor yoke surface (R_r)	40 mm

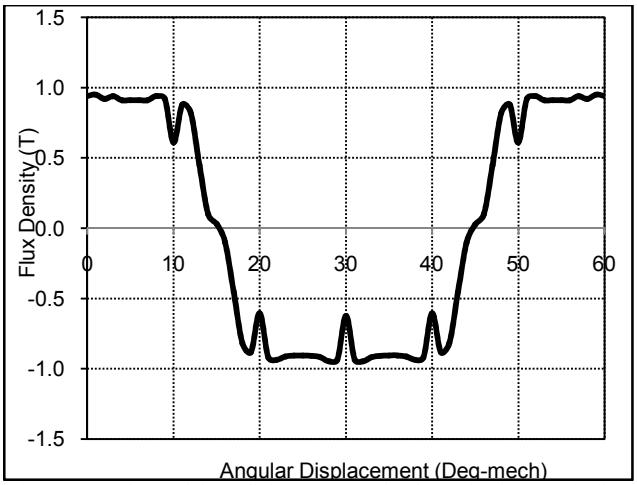

Fig. 2. Waveform of the radial component for the no load magnetic flux density in the air-gap under one pole pitch (Analytical Result).

C. FE Optimization and Results

There are lots of methods available in literature [7-8] for the reduction of cogging torque in slotted motors. The most significant methods among them are: i) skewing of the stator slots or PMs, ii) change in magnet pole-arc to pole-pitch ratio, iii) providing notches in stator teeth, iv) shifting of PM pole pairs and v) adopting fractional slot pitch combination. The research done by the authors [9] clearly revealed the advantages of adopting fractional slot pitch configuration for reducing cogging torque in slotted PMBLDC motors. The number of cogging cycles in one complete mechanical rotation is given by the least common multiple of the number of stator slots (i.e., Q_s) and the number of poles (i.e., $2p$).

When the frequency of the cycle increases, the peak amplitude of the cogging torque comes down. Based on this strategy, the 12 poles, 36 slots experimental motor designed analytically is analyzed using FE with stator of different slot numbers. From the FE analysis it was clear that the cogging torque reduces drastically once 37 slots was selected in the stator instead of 36. The Fig. 4 shows a comparison of the developed torque pattern under one pole pitch for a 36 slots and 37 slots radial magnetized PMBLDC motor. The torque

pulsation in the developed torque is very high for a 36 slots combination which is detrimental for the positional stability for precise space applications. But the developed torque pattern has the least torque pulsations when a 37 slots combination is adopted. The Fig. 5 shows the cogging torque pattern of a 36 slots and 37 slots combinations.

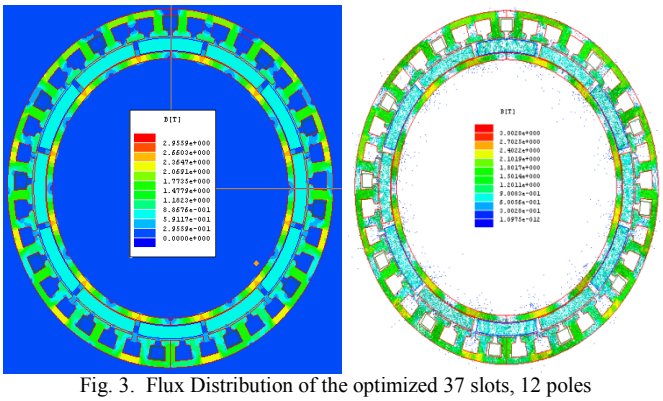

Fig. 3. Flux Distribution of the optimized 37 slots, 12 poles PMBLDC motor (FE Results)

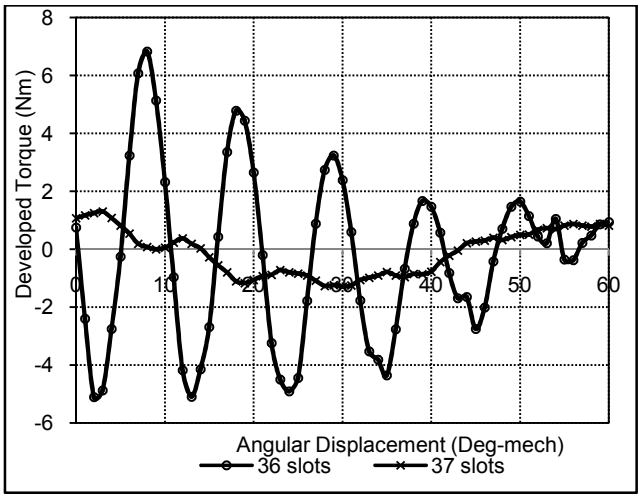

Fig. 4. Comparison of the developed torque patterns of a 12 poles, 36 slots and 37 slots PMBLDC motor (FE Results).

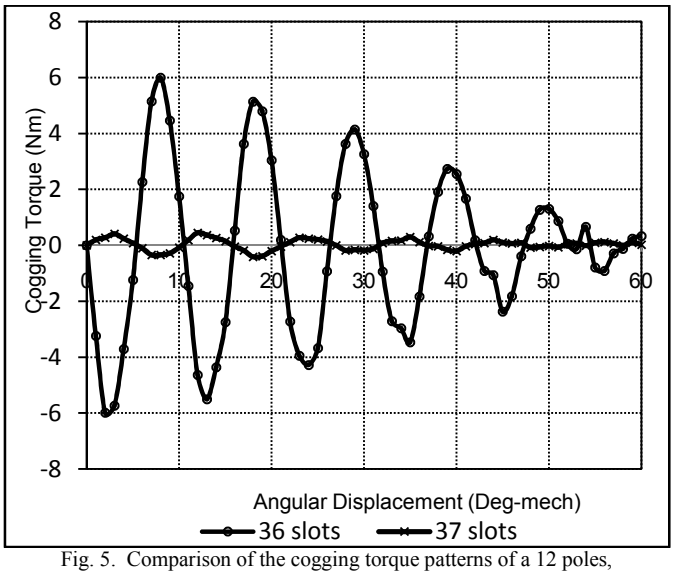

Fig. 5. Comparison of the cogging torque patterns of a 12 poles, 36 slots and 37 slots PMBLDC motor (FE Results).

The magnitude of the cogging torque is very much reduced in a 37 slots combination when compared to a 36 slots PMBLDC motor. The machine is found to develop a peak developed torque of 1.3 Nm and an average torque of 0.723 Nm. But the magnitude of cogging torque even in the optimized model (37 slots, 12 poles) is found to be 20 % of the developed torque which is higher than that of a hybrid stepper motor of compatible size. Hence in order to suit the spacecraft application requirements another class of PMBLDC motors, i.e., a slotless PMBLDC configuration is investigated. The use of ferromagnetic material on the rotor can be avoided in a Halbach machine unlike that of radial and parallel magnetization [10] thereby reducing the core losses and permitting high torque to inertia ratio. Hence slotless Halbach air core PMBLDC machine is considered for further analysis.

III. Analysis of a Slotless PMBLDC Motor

A. Analytical Modeling

For deriving the analytical model of a slotless Halbach magnetized PMBLDC motor, scalar magnetic potentials derived from the solutions of Laplace's and Poisson's equations is used. In order to obtain analytical solution for the field distribution produced in a multi-pole Halbach machine, the following assumptions are made: i) the PM is oriented according to Halbach magnetization and is fully magnetized in the direction of magnetization; ii) the effect of finite axial length is neglected; iii) the back iron is infinitely permeable.

The Fig. 6 shows a zero cogging PMBLDC motor with Halbach array. Unlike that of conventional slotted type PMBLDC motor, the zero cogging PMBLDC motor employs slotless stator winding. Concentrated type of winding is employed as it gives less end winding and avoids overlapping of phase windings. The inherent self shielding property of Halbach machines over radial and parallel magnetized machines makes it an ideal choice for employing coreless configuration. From the schematic diagram of the machine shown in Fig.6 the region inside the Halbach array is considered as air as coreless machine configuration is

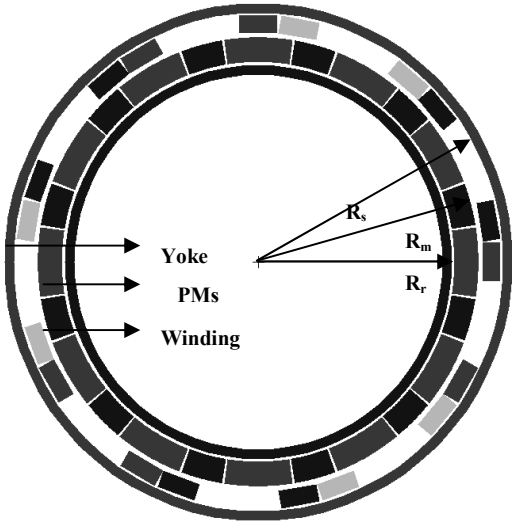

Fig. 6. Zero cogging PMBLDC Motor with Halbach array.

considered which suits space requirements. Hence the complete solution for the internal rotor Halbach array zero cogging motor under study is obtained by the solution of Laplace's and quasi-Poisson's equation in the air-gap and in the PMs respectively and by the application of boundary conditions. The final mathematical model for the internal rotor zero cogging Halbach array motor has been developed in [11-12]. The radial component of the magnetic flux density in the air-gap is defined by

$$B_{r1} = -\frac{4p \cdot B_{rm}}{M_0 \cdot (1+\mu_{rm})} \cdot \frac{1}{(1+p)} \cdot \left[1 - \left(\frac{R_r}{R_m}\right)^{p+1}\right] \cdot \left[\left(\frac{r}{R_s}\right)^{p-1} \cdot \left(\frac{R_m}{R_s}\right)^{p+1} + \left(\frac{R_m}{r}\right)^{p+1}\right] \cdot \cos\left(p \cdot \Theta_s\right), \quad (7a)$$

$$M_0 = 2 \cdot \left\{ \begin{array}{l} \left(\frac{1-\mu_{rm}}{1+\mu_{rm}}\right)^2 \cdot \left(\frac{R_r}{R_m}\right)^{2p} - 1 \\ -\left[1 - \left(\frac{R_r}{R_m}\right)^{2p}\right] \cdot \frac{(1-\mu_{rm})}{(1+\mu_{rm})} \cdot \left(\frac{R_m}{R_s}\right)^{2p} \end{array} \right\}, \quad (7b)$$

where μ_{rm} is the relative recoil permeability of the PMs, R_r is the internal radius of the magnet, R_m is the magnet outer radius, R_s is the stator outer bore radius. A code was developed in MATLAB based on the analytical model developed for Halbach array slotless PMBLDC motor. They are formulated in polar coordinates and account for relative recoil permeability of the PMs.

B. Analytical Results and Discussion

The analytical expressions given in (7) is used for computing the radial component of the mean magnetic flux density in the air-gap for a Halbach slotless internal rotor PMBLDC motor with the required specifications of (104x40) mm. The Fig. 7 shown below gives the variation of peak air gap flux density at mean air gap radius with pole pair number of the Halbach slotless air core PMBLDC machine to be designed. The length of the magnetic flux path in a Halbach magnetized rotor is dependent on the pole pair number and hence there exist an optimum number of poles at which the flux density is maximum. The same is not applicable for radial and parallel magnetized machines since the length of the magnetic flux is constant (equal to the magnetic thickness) [13]. It can be seen from Fig. 7 that the optimum flux density is obtained when the total number of rotor poles is selected as 12. With the increase in length of the PM even though the mean air gap flux density increases the space available for accommodating the stator windings decreases. Hence based on the tradeoff between electrical and magnetic loading optimized values of length of PM and pole pairs are chosen as 6 and 12 mm respectively. The Fig. 8 shows variation of the mean air gap flux density under one pole pitch of the Halbach slotless air core PMBLDC designed. Unlike that of a slotted PMBLDC motor configuration, the flux density waveform at

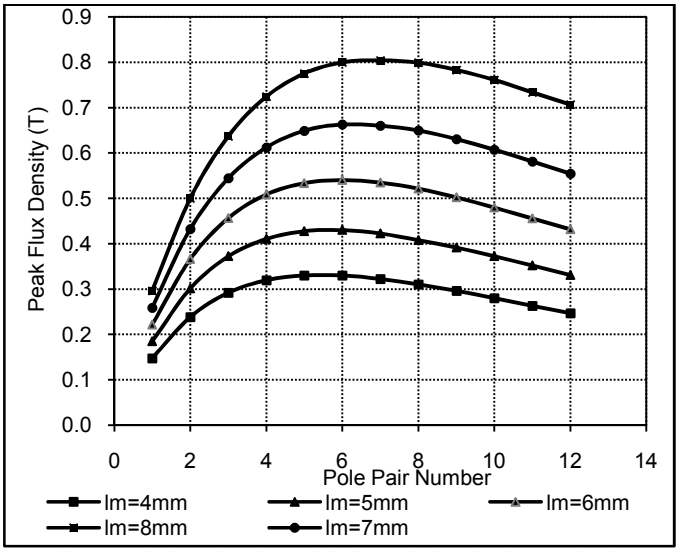

Fig. 7. Variation of peak B_{r1} with change in length of PM and pole pairs (Analytical Results).

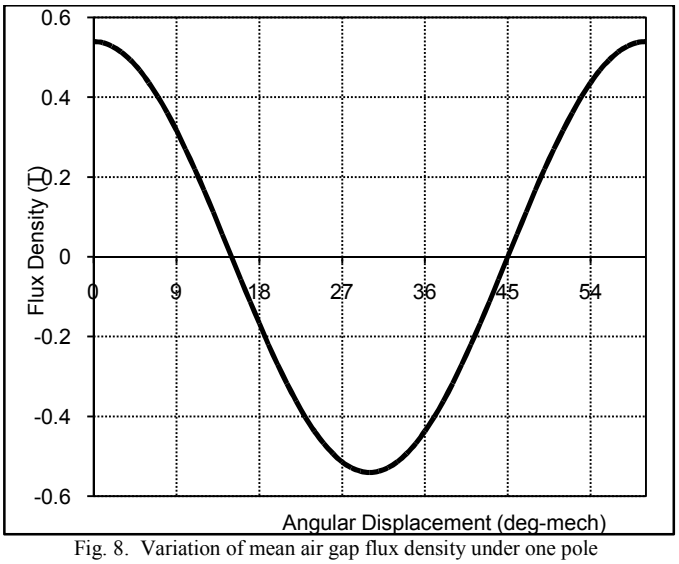

Fig. 8. Variation of mean air gap flux density under one pole pitch (Analytical Results).

the mean air gap of a Halbach array slotless motor is free of any harmonic content .This is due to the adoption of slotless topology. Also this design is free of the cogging torque component as stator is having no teeth. Hence a zero cogging Halbach array PMBLDC motor is designed which largely suits spacecraft applications.

A brief design data of the developed zero Cogging Halbach array PMBLDC motor is given in Table 2.

C. FE Results and Discussion

The basic design parameters obtained from the analytical results of a slotless PMBLDC motor with Halbach array, such as the length of the PM and the number of pole pairs is used to model the machine in FE. The 2-D FE analysis is carried out as the machine is axisymmetric. The commercial FE Software package, i.e., Maxwell 2-D, is used for the analysis. The Fig. 9 shows the flux density plot and the magnetic vector plot of the designed zero cogging Halbach motor. From the flux pattern, it is clear that flux focusing PM acts as a path for flux

TABLE II
DESIGN DETAILS OF THE HALBACH ARRAY SLOTLESS PMBLDC MOTOR

Parameter	**Value**
Dimension	Φ(104x 40)mm
Supply voltage	28 V
No. of phases (m)	3
No. of poles ($2p$)	12
No. of stator coils	9
Resistance/Phase	3.37 Ω
Air-gap thickness	0.5 mm
Permanent magnet	Sm_2CO_{17}
No. of PMs	12+12
Axial length of PMs	30 mm
Position sensor	Hall element
Magnet thickness	6 mm
Radius of the stator surface (R_s)	50 mm
Radius of the PM's surface (R_m)	44 mm
Radius of the rotor yoke surface (R_r)	38 mm

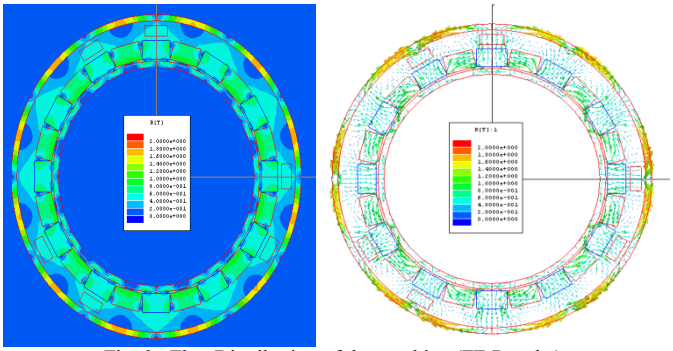

Fig. 9. Flux Distribution of the machine (FE Results).

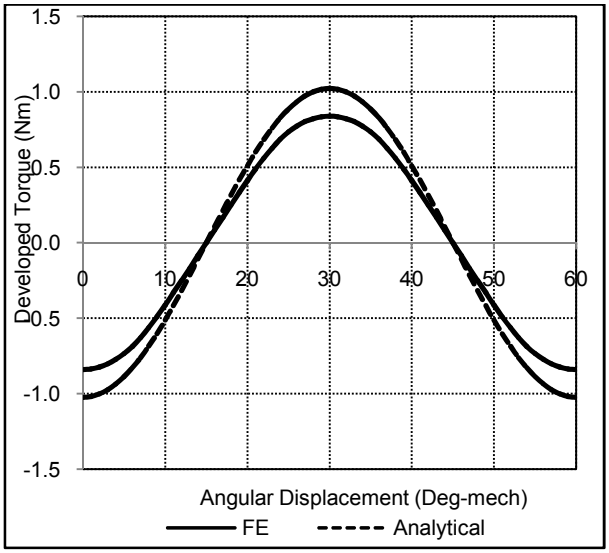

Fig. 10. Comparison of the developed torque patterns obtained from analytical and FE Results.

between adjacent poles and hence reduces the flux in the back iron. The Fig. 10 gives a comparison of the torque developed by the machine at 1 A excitation obtained from analytical and FE results. FE results are found to be in close agreement to that obtained from analytical results. The slight discrepancy between the results can be attributed to the realization of the Halbach array using discrete magnet segments.

The zero cogging Halbach array PMBLDC motor designed is found to develop a peak torque of 0.84 Nm at 1 A excitation and an average torque of 0.55 Nm under one pole pitch.

TABLE III
COMPARISON OF PMBLDC MACHINE CONFIGURATIONS

Configuration	Average Torque (Nm)	Peak Torque (Nm)	Cogging Torque (%)
Slotted PMBLDC Motor	0.72	1.3	20
Slotless Halbach array PMBLDC Motor	0.55	0.84	0

IV. COMPARISON OF SLOTTED AND SLOTLESS PMBLDC MACHINE CONFIGURATIONS

Two different types of surface mounted PMBLDC machine configurations such as a radial magnetized slotted PMBLDC machine and Halbach magnetized slotless PMBLDC machine of same dimensions are analyzed using FE and analytical results. The Table 3 gives a comparison of the torque developed in the machines and it is found that slotless topology eliminates the cogging component of the torque completely without much reduction the developed torque component. Hence a slotless Halbach array PMBLDC motor topology is found to be the best topology to cater the needs for precise spacecraft applications.

V. CONCLUSION

The optimal design of a surface mounted PMBLDC meant for spacecraft applications is carried out. Two types of machine configurations such as slotted PMBLDC and slotless PMBLDC with Halbach array were compared with analytical and FE results. It is found that unlike that of slotted PMBLDC motor a slotless PMBLDC motor with Halbach array develops zero cogging torque without much reduction in the developed torque. Moreover the use of Halbach array helps in achieving high Torque to inertia ratio and reduces core losses. The machine being coreless has zero magnetic stiction. The optimal design of Slotless Halbach Array PMBLDC machine is found to develop a peak torque of 0.84 Nm at 1 A excitation and meet the required design requirements for spacecraft applications.

VI. ACKNOWLEDGMENT

The authors would like to thank Indian Space Research Organisation Inertial Systems Unit, Department of Space, Government of India, M/s Cochin University of Science & Technology, Kerala, India and M/s College of Engineering, Trivandrum, Kerala, India and M/s University of Franche-Comte (UFC), Belfort, France for their help with this project.

VII. REFERENCES

[1] "*Selection of Electric Motors for Aerospace Applications*", NASA Document on Preferred Reliability Practices, Practice No. PD-ED-1229, pp. 1-6.

[2] F. Dubas and C. Espanet, "*Semi-Analytical Solution of Cogging Torque in SMPMM*", IEEE COMPUMAG'09 Conference, Florianopolis, Brasil, November 2009.

[3] R.P. Praveen, M.H. Ravichandran *et.al*; "*Design and Finite Element Analysis of Hybrid Stepper motor for Spacecraft Applications"*, IEEE IEMDC, pp. 1051-1057, May 2009.

[4] T. Kenjo and S. Nagamori, "*Permanent Magnet and Brushless DC Motors*", Clarendon Press, Oxford, 1985.

[5] T.J.E. Miller, "*Brushless Permanent Magnet and Reluctance Motor Drives*", Clarendon Press, Oxford, 1989.

[6] F. Dubas and C. Espanet, "*Analytical Solution of the magnetic field in permanent magnet motors taking in to account slotting effect: No-load vector potential and flux density calculation*", IEEE Trans. on Magn., vol. 45, no. 5, pp. 2097–2109, May 2009.

[7] T. Li, G. Slemon, "*Reduction of Cogging torque in permanent magnet motors*", IEEE Trans. on Magn., vol. 24, no 6, pp. 2901-2903, November 1988.

[8] M. Dai, A. Keyhani, T. Sebastin, "*Torque Ripple Analysis of a PM Brushless DC Motor using finite Element Method*", IEEE Trans. on Energy Conv., vol 19, no. 1, pp. 40-45, March 2004.

[9] M.H. Ravichandran, V.T. Sadasivan Achari *et.al*., "*Remedial strategies for the minimization of cogging Torque in PMBDC motor possessing material saturation*", IEEE PEDES, pp. 1-4, December 2006.

[10] R.P. Praveen, M.H. Ravichandran *et.al*., "*Design and Analysis of Zero Cogging Brushless DC motor for Spacecraft Applications"*, IEEE ECTI-CON, pp. 254 -258, May 2010.

[11] R.P. Praveen, M.H. Ravichandran *et.al*., "*Design and Analysis of Enclosed Rotor Halbach Array Brushless DC motor for Spacecraft Applications"*, IEEE ICEM'10 Conference, Rome, Italy, pp. 1 -6, September 2010.

[12] Z.P. Zia and Z.Q. Zhu, "*Analytical Magnetic Field Analysis of Halbach Permanent magnet machines*", IEEE Trans. on Magn., vol. 40, no. 4, pp. 1864-1872, June 2004.

[13] S.M. Jang, S.S. Jeong, "*Comparison of three types of PM Brushless machines for an electro-mechanical battery*", IEEE Trans. on Magn., vol. 36, no. 5, pp. 3540-3543, Sept. 2001.